ORGANIC CHEMISTRY FRONTIERS

RESEARCH ARTICLE

View Article Online
View Journal

Cite this: DOI: 10.1039/d5qo01184a

Bis-guanidinate magnesium amide-catalyzed hydroboration of nitriles and isocyanides *via* a substrate-assisted pathway

Sayantan Mukhopadhyay, Smrutirani Padhan, Anubhab Das and Sharanappa Nembenna *

Received 16th August 2025,
Accepted 23rd October 2025

DOI: 10.1039/d5qo01184a

rsc.li/frontiers-organic

The bis-guanidinate amido magnesium(II) compound [LMgN(SiMe$_3$)$_2$; L = {(ArHN)(ArN)–C=N–C = (NAr)(NHAr)}; [Ar = 2,6-Et$_2$-C$_6$H$_3$] (**Mg-1**) has been employed as a pre-catalyst for the dihydroboration of nitriles, and as a catalyst for the dihydroboration of isocyanides, affording *N*,*N*-bis(boryl)amines and *N*,*C*-di(boryl)amines in good yields. The protocol introduces the first examples of nitrile and isocyanide reduction *via* a substrate-assisted pathway. The active catalyst for nitrile hydroboration, LMg-N(SiMe$_3$)$_2$·3-Me-C$_6$H$_4$CN (**Mg-2**), and the intermediate for isocyanide reduction, LMg-N(SiMe$_3$)$_2$·2,6-Me$_2$-C$_6$H$_3$NC (**Mg-3**), were isolated and thoroughly characterized by multinuclear NMR spectroscopy and single-crystal X-ray diffraction. Based on these findings, plausible mechanistic cycles for both nitrile and isocyanide dihydroboration reactions have been proposed.

Introduction

The reduction of nitriles (R–C≡N) and isocyanides (R–N=C) plays a pivotal role in synthetic chemistry.[1–3] This process yields primary amines from nitriles and secondary amines from isocyanides, both of which are highly valuable due to their extensive applications. These compounds serve as essential feedstocks for agrochemicals, pharmaceuticals, dyes, and drug production, making them vital to industry and a key focus for synthetic chemists.[4–13]

Traditional ways for this kind of reduction include treatment of nitriles with metal hydrides,[14] which may involve potential drawbacks such as use of pyrophoric and expensive reagents, poor selectivity,[15,16] and direct hydrogenation with combustible hydrogen gas,[17] which requires harsh reaction conditions[18] often concerning about safety issues. In this context, metal-catalyzed hydroboration has proved to be more advantageous over traditional stoichiometric synthetic procedures by producing higher selectivity, milder reaction conditions, and reduced waste generation, and has emerged as a new alternative towards the reduction of various unsaturated organic moieties.[13,19–24] Metal-catalyzed B–H or Si–H additions to the unsaturated organic functionalities are highly dominated by molecular metal hydrides following a hydride pathway;[14,25] however, a few examples of hydride-free pathway are also reported.[26–28] Despite extensive studies on transition,[1,13,29–48] main group,[1,48–65] and rare earth metal catalyzed[1,48,66] hydroboration of nitriles and isocyanides, reports on magnesium-catalyzed hydroboration of the same, which remained scarce.[56,57,63]

Magnesium, being eco-friendly, non-toxic, earth-abundant, and biocompatible,[67–71] offers significant potential in this domain. However, despite numerous advancements in the catalytic as well as stoichiometric applications of magnesium-based complexes,[1,21,28,72,73] only three studies have explored its catalytic application in hydroboration of nitriles[57] and isocyanides,[63] underscoring a critical gap in this field.

The first report on metal-catalyzed nitrile dihydroboration was documented by the Nikonov group in 2012 using a molybdenum-based catalyst, (2,6-^{i}Pr$_2$-C$_6$H$_3$N)Mo(H)(Cl)(PMe$_3$)$_3$.[43] In 2016, the Hill group introduced a β-diketiminate (Nacnac) magnesium complex, [CH{C(Me)NAr}$_2$Mg-*n*Bu] (Ar = 2,6-^{i}Pr$_2$C$_6$H$_3$), as a pre-catalyst for nitrile hydroboration, representing the first example with magnesium (Fig. 1). Notably, the same group reported the first metal-catalyzed hydroboration of isocyanides in 2015 using the same pre-catalyst, with both cases involving *in situ* generation of magnesium hydride species as the active catalyst. In 2018, Ma and coworkers reported unsymmetrical-diketiminate-stabilized Mg(I) dimer catalyzed double hydroboration of nitriles, though they couldn't mention any mechanistic insights on the catalytic transformation.[56]

Recently, the Trovitch group reported cobalt-catalyzed nitriles dihydroboration,[38] in which authors introduced a chelate-assisted hydroboration pathway. To our knowledge,

School of Chemical Sciences, National Institute of Science Education and Research (NISER), HBNI, Bhubaneswar, 752 050, India. E-mail: snembenna@niser.ac.in

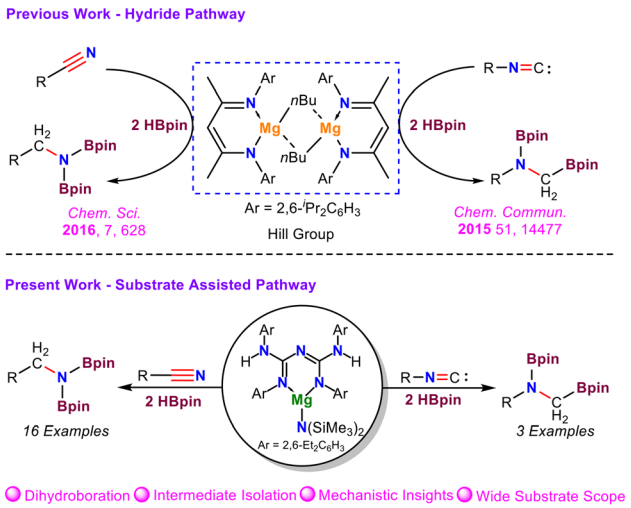

Fig. 1 Magnesium-catalyzed dihydroboration of nitriles and isocyanides.

there have been no reports on the magnesium catalyzed hydroboration of nitriles and isocyanides involving chelate- assisted or substrate-driven pathway. This scarcity of studies on magnesium-catalyzed hydroboration of nitriles and isocyanides *via* substrate-assisted pathway, coupled with limited mechanistic insights, underscores the need to design innovative magnesium complexes and explore alternative pathways to unlock the full potential of this catalytic transformation.

In this context, we employed bis-guanidinate Mg(II) amide [LMgN(SiMe$_3$)$_2$] (**Mg-1**)[74] as a pre-catalyst for the hydroboration of the nitriles and a catalyst for the dihydroboration of isocyanides with good to excellent yields. We have isolated and characterized the active species LMg-N(SiMe$_3$)$_2$·3-Me-C$_6$H$_4$CN (**Mg-2**), and LMg-N(SiMe$_3$)$_2$·2,6-Me$_2$-C$_6$H$_3$NC (**Mg-3**) with various spectroscopic techniques (^{1}H, ^{13}C{^{1}H}, ^{29}Si{^{1}H}) and XRD analysis. Moreover, based on the above findings, we established the first example of amido magnesium complex-catalyzed hydroboration of nitriles and isocyanides, with a mechanistic insight into the substrate-assisted pathway.

Results and discussion

Dihydroboration of nitriles

Our group previously developed a "Nacnac" analogue – specifically, a tetra-*N*-aryl substituted bis-guanidine ligand and its coordination chemistry.[64,75,76] Recently, we synthesized bis-guanidinate magnesium amide complex (**Mg-1**) and employed it as a catalyst for the C–C coupling of terminal alkynes with carbodiimide (CDI) (Fig. 2).[74]

Inspired by the work of the Hill group on magnesium-catalyzed dihydroboration of nitriles,[57] we investigated the use of **Mg-1** as a pre-catalyst for nitrile dihydroboration. Our initial experiment began with *m*-tolunitrile (**1c**) as a model substrate and pinacolborane (HBpin) as a hydroborating agent, to optimize the catalytic transformation. A control reaction without a

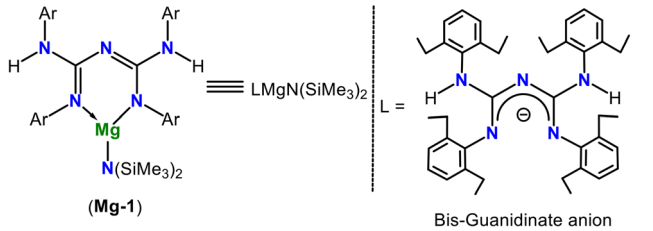

Fig. 2 Bis-guanidinate stabilized Mg(II) amide (**Mg-1**).

catalyst, performed at 80 °C for 24 h under neat conditions, showed no conversion. However, under identical conditions, the presence of 5 mol% of **Mg-1** afforded quantitative conversion to the corresponding *N*,*N*-bis(boryl)amine (**2c**), confirmed by ^{1}H NMR spectroscopy (Table 1, entry 2). Reducing the catalyst loading to 1 mol% under neat conditions at 60 °C achieved full conversion within 12 h (Table 1, entry 4). Further decrease in the reaction time led to reduced NMR conversions (Table 1, entries 5 and 6).

The same reaction produced quantitative conversion upon heating at 60 °C for 14 h in C$_6$D$_6$ (Table 1, entry 11). Additionally, we tested the activity of **Mg-2** (*vide infra*) for the dihydroboration reaction, which produced quantitative conversion at 80 °C, within 10 h in C$_6$D$_6$ (Table 1, entry 12). We also tested the catalytic activity of magnesium bis(trimethylsilyl)amide [Mg{N(SiMe$_3$)$_2$}$_2$][77] reagent, which showed only 10% conversion to the diborylated product (Table 1, entry 13),

Table 1 Optimization table of magnesium catalyzed dihydroboration of *m*-tolunitrile[a]

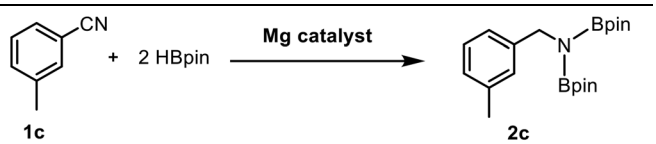

Entry	Cat.	mol%	Solvent	Temp. (°C)	Time (h)	Conv.[b] (%)
1	—	—	Neat	80	24	—
2	**Mg-1**	5	Neat	80	24	>99
3	**Mg-1**	3	Neat	70	12	>99
4	**Mg-1**	**1**	**Neat**	**60**	**12**	**>99**
5	**Mg-1**	1	Neat	60	11	94
6	**Mg-1**	1	Neat	60	6	55
7	**Mg-1**	1	Neat	rt	24	30
8	**Mg-1**	0.5	Neat	60	12	75
9	**Mg-1**	0.5	Neat	60	24	75
10	**Mg-1**	0.5	Neat	80	24	75
11	**Mg-1**	1	C$_6$D$_6$	60	14	>99
12	**Mg-2**	1	C$_6$D$_6$	60	10	>99
13	Mg[N(SiMe$_3$)$_2$]$_2$	1	Neat	60	12	10

[a] Reaction conditions: *m*-tolunitrile (0.1 mmol, 1.0 equiv.), pinacolborane (HBpin) (0.2 mmol, 2.0 equiv.), catalyst **Mg-1**, **Mg-2** and **Mg[N(SiMe$_3$)$_2$]$_2$** (*x* mol%). [b] Conversions for the reduction of *m*-tolunitrile to *N*,*N*′-bis-borylated amine were examined by ^{1}H and ^{13}C{^{1}H} NMR spectroscopy based on the consumption of starting material and formation of characteristic new proton resonance for {C*H*$_2$N(Bpin)$_2$} moiety.

highlighting the superior activity of a heteroleptic molecular magnesium complex like **Mg-1**, over a homoleptic magnesium complex [Mg{N(SiMe$_3$)$_2$}$_2$]. Further reduction in catalyst loading led to decreased conversions, even at elevated temperature and prolonged reaction time (Table 1, entries 7–10).

With optimized reaction conditions in hand, we explored the substrate scope. A variety of nitriles (**1a–1p**), including electron-donating (**1a–1g**), electron-withdrawing (**1h–1n**) substituted aryl nitriles, as well as alkyl nitriles (**1o**, **1p**), were successfully dihydroborated with HBpin in the presence of **Mg-1**. The corresponding *N*,*N*-bis(boryl)amines (**2a–2p**) were obtained with quantitative conversion (Table 2) except for **2p** (88%). Nitrile **1a** underwent complete conversion to **2a** within 6 h. To probe substituent effects, we examined **1c** (electron-donating) and **1m** (electron-withdrawing) under shorter reaction times (<12 h), which resulted in comparatively lower conversions (11 h, ~90%). Based on these observations, subsequent substrates were screened under standardized overnight heating (up to 12 h), ensuring quantitative conversions. Furthermore, to assess the effect of electronic substitution on the initial rate, we monitored the hydroboration of **1c** and **1m** at 3 h under optimal conditions in C_6D_6 (see SI, Fig. S20 and S42). Both substrates displayed nearly identical NMR conversions (32–34%), indicating comparable initial reaction rates. These observations suggest that electronic effects of the substituents have little influence on the reaction rate, and the reduced rates in the substituted nitriles are instead attributed to steric hindrance during catalyst–substrate complex formation (see stoichiometric reactions). The aliphatic nitrile **1o** gave >99% NMR conversion, while its aryl analogue **1p** gave a slightly lower yield (88%). All products were characterized by ^{1}H and ^{13}C{^{1}H} NMR spectroscopy. New signals in the range of 2.86–4.38 ppm in the ^{1}H NMR spectra, corresponding to the C*H*$_2$N(Bpin)$_2$ moiety, confirmed successful conversion. The yield of **2p** was determined using mesitylene as an internal standard [see SI, Fig. S47 and S48].

Table 2 Substrate scope for **Mg-1** catalyzed dihydroboration of nitriles[a,b,c]

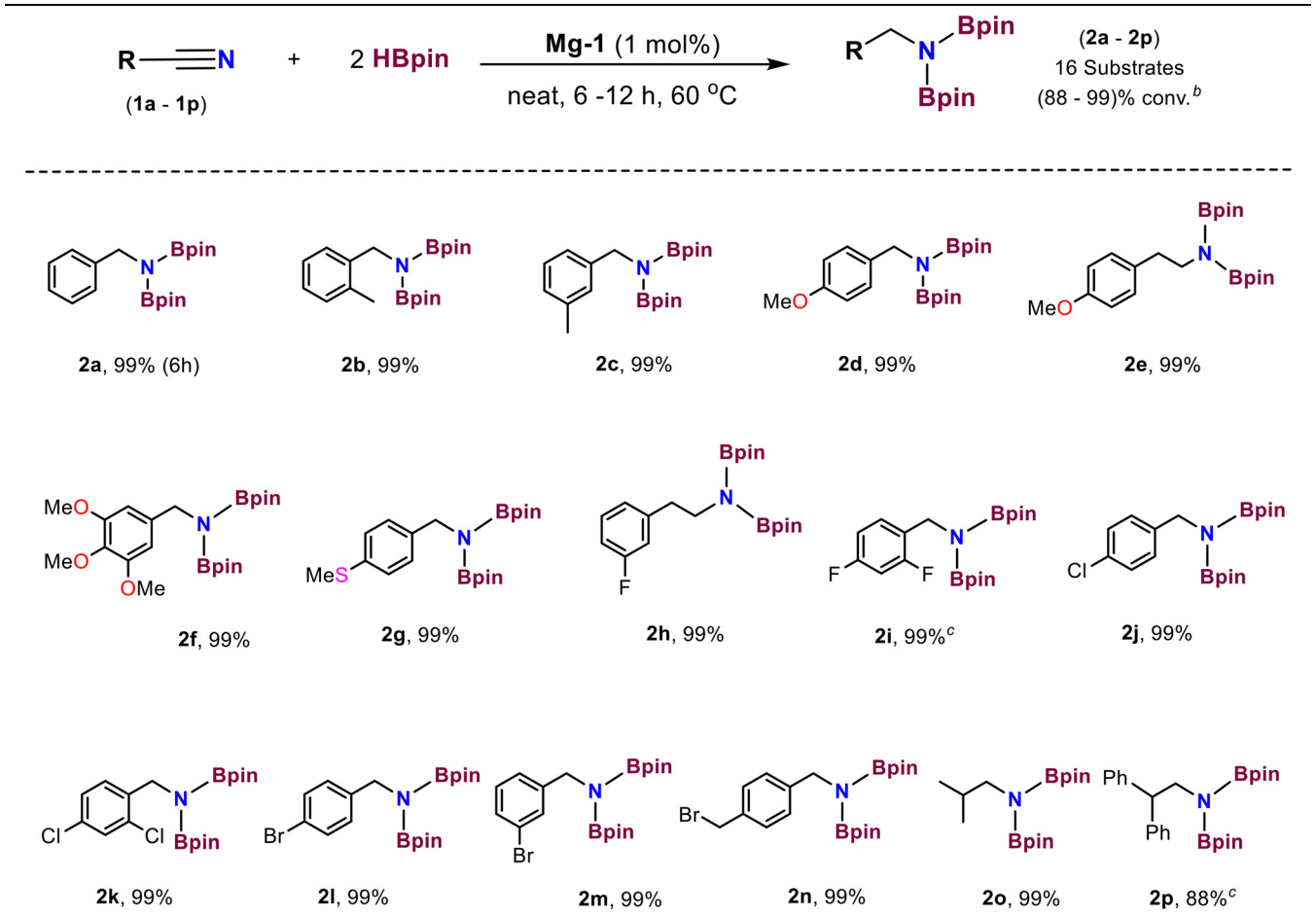

[a] Reaction conditions: nitriles (0.2 mmol, 1.0 equiv.), pinacolborane (HBpin) (0.4 mmol, 2.0 equiv.), catalyst **Mg-1** (1 mol% %), heating at 60 °C, 12 h (6 h for **1a**) stirring under neat conditions. [b] Conversion for the product was examined by ^{1}H and ^{13}C{^{1}H} NMR spectroscopy based on the consumption of starting material and formation of characteristic new proton resonance for the (CH$_2$N(Bpin)$_2$) moiety of products **2a–2p**. [c] For compounds **2i** and **2p**, mesitylene is used as an internal standard.

Dihydroboration of isocyanides

Encouraged by our success with nitriles and noting the limited reports on isocyanide hydroboration,[62,63] we evaluated the catalytic activity of **Mg-1** for the dihydroboration of isocyanide. Using 2,6-dimethylphenyl isocyanide (**3a**) as a model substrate, a catalyst-free reaction with HBpin at 80 °C for 24 h in benzene-d_6 yielded no conversion (Table 3, entry 1). In contrast, using 10 mol% **Mg-1** resulted in quantitative formation of *N*,*C*-di(boryl)amine (**4a**) (Table 3, entry 2), as confirmed by ^{1}H NMR spectroscopy. Decreasing the catalyst loading to 6 mol% still provided full conversion at 70 °C within 12 h (Table 3, entry 4). The same reaction showed no change in the NMR conversion under neat conditions (Table 3, entry 5). Further reduction in the catalyst load decreased the conversion significantly (Table 3, entry 6). The reagent $Mg[N(SiMe_3)_2]_2$[77] produced only 30% conversion under standard reaction conditions (Table 3, entry 7).

Next, we investigated other isocyanides: 2-naphthyl isocyanide (**3b**) showed 70% conversion to **4b**, while cyclohexyl isocyanide (**3c**) underwent complete conversion to **4c** (Table 3).

Table 3 Optimization table of magnesium catalyzed hydroboration of isocyanide[a,b,c]

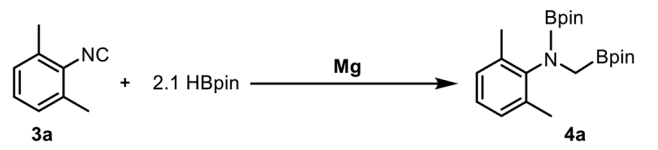

Entry	Cat	mol%	Solvent	Temp. (°C)	Time (h)	Conv.[b] (%)
1	—	—	C_6D_6	80	24	—
2	Mg-1	10	C_6D_6	80	24	>99
3	Mg-1	7	C_6D_6	70	12	>99
4	**Mg-1**	**6**	$\mathbf{C_6D_6}$	**70**	**12**	**>99**
5	Mg-1	6	Neat	70	12	>99
6	Mg-1	5	C_6D_6	70	24	80
7	$Mg[N(SiMe_3)_2]_2$	6	C_6D_6	70	12	30

Substrate Scope[c]

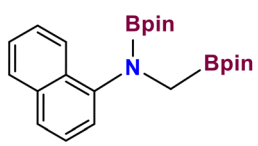

4b, 70%

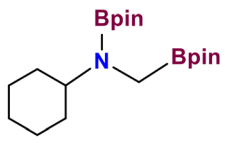

4c, >99%

[a] Optimization reaction conditions: 2,6-dimethylphenyl isocyanide (**3a**) (0.1 mmol, 1.0 equiv.), pinacolborane (HBpin) (0.21 mmol, 2.1 equiv.), catalyst **Mg-1** or $\mathbf{Mg[N(SiMe_3)_2]_2}$ (*x* mol%). [b] Conversion of **3a** to the corresponding 1,2-diborylated amine (**4a**) was examined by ^{1}H and ^{13}C{^{1}H} NMR spectroscopy based on the consumption of starting material and formation of characteristic new proton resonance for the {CH_2N(Bpin)$_2$} moiety. [c] Reactions were performed with **3b** and **3c** (0.1 mmol, 1.0 equiv.), pinacolborane (HBpin) (0.21 mmol, 2.1 equiv.), catalyst **Mg-1** (**6 mol%**), heated at 70 °C, for 12 h. Conversions to 1,2-diborylated amines (**4b**, **4c**)were examined by ^{1}H and ^{13}C{^{1}H} NMR spectroscopy based on the formation of a characteristic new proton resonance for {CH_2(Bpin)N(Bpin)} moiety.

These products were confirmed by ^{1}H and ^{13}C{^{1}H} NMR spectroscopy. New singlets in the 2.74–3.61 ppm range, attributed to the N(Bpin)CH_2Bpin moiety, confirmed successful formation (see SI). We attempted dihydroboration of isocyanide substrates **3d**, **3e**, and **3f**; however, the corresponding borylated products **4d**, **4e**, and **4f** were obtained in low conversions (SI, Table S1).

Stoichiometric reactions for the hydroboration of nitriles and isocyanides

To gain mechanistic insights into the bis-guanidinate magnesium amide-catalyzed hydroboration reactions of nitriles and isocyanides, we executed a series of control experiments. Previously, the Hill group reported β-diketiminate (Nacnac) stabilized magnesium alkyl as a pre-catalyst for the hydroboration of organic nitriles,[57] involving the *in situ* formation of magnesium hydride. It is worthy to note, that molecular magnesium hydrides can be accessed by the reaction between magnesium amide and silane reagents,[14,78–84] however, a 1 : 3 stoichiometric reaction of **Mg-1** and HBpin at 90 °C for 24 h indicated the formation of the **Mg1**-HBpin adduct in the ^{1}H NMR spectrum (see SI, Fig. S7) (Scheme 1i). In addition, we observed no conversion of HBpin into BH_3 in the presence of **Mg-1** (see SI, Fig. S13) which rules out the any hidden catalysis[85,86] for the hydroboration reactions. A 1 : 1 stoichiometric reaction between **Mg-1** and *m*-tolunitrile (**1c**) in C_6D_6 produced the monomeric nitrile coordinated adduct LMg-N$(SiMe_3)_2$·3-Me-C_6H_4CN **Mg-2** within 5 min of the reaction at room temperature (Scheme 1ii). The compound **Mg-2** was isolated and characterized by multinuclear NMR spectroscopy and single-crystal X-ray diffraction analysis. The ^{1}H NMR spectrum of the compound **Mg-2** displayed a downfield shift of the methyl groups of the N$(SiMe_3)_2$ moiety at 0.35 ppm than its parent precursor **Mg-1** at 0.01 ppm in C_6D_6,[74] indicating the coordination of the electron-withdrawing nitrile group. A considerable downfield shift has been observed for the Ar–N*H* moiety of the ligand backbone at 5.03 ppm (**Mg-1**; Ar–N*H*: ^{1}H NMR δ 4.89 ppm) in the ^{1}H NMR spectrum, indicating the **Mg-2** formation. ^{13}C{^{1}H} NMR spectrum also displayed a significant shift of the N$(SiMe_3)_2$ carbons at 5.7 ppm than the **Mg-1** at 4.4 ppm in C_6D_6 [see SI, Fig. S2]. Additionally, one singlet signal at −7.93 ppm in the ^{29}Si{^{1}H} NMR spectrum shows a slight shift from its parent precursor at −7.22 ppm in C_6D_6, indicating the formation of the new species **Mg-2** [see SI, Fig. S1, S2, and S3].

Though some isocyanide adducts of ligated magnesium complexes are reported in the literature,[87] to our knowledge, **Mg-2** is the first example of a nitrile adduct of a bis-guanidinate-stabilized magnesium amide complex. The single crystals suitable for X-ray diffraction analysis were grown inside a J. Young valve NMR tube in C_6D_6 at room temperature. The X-ray diffraction study shows that the compound crystallizes in a monoclinic system with a $P2_1/n$ space group. The molecular structure shows a monomeric unit with a magnesium centre surrounded by four N atoms: two from the chelated bis-guanidinate ligand, and others from the N$(SiMe_3)_2$ and the nitrile

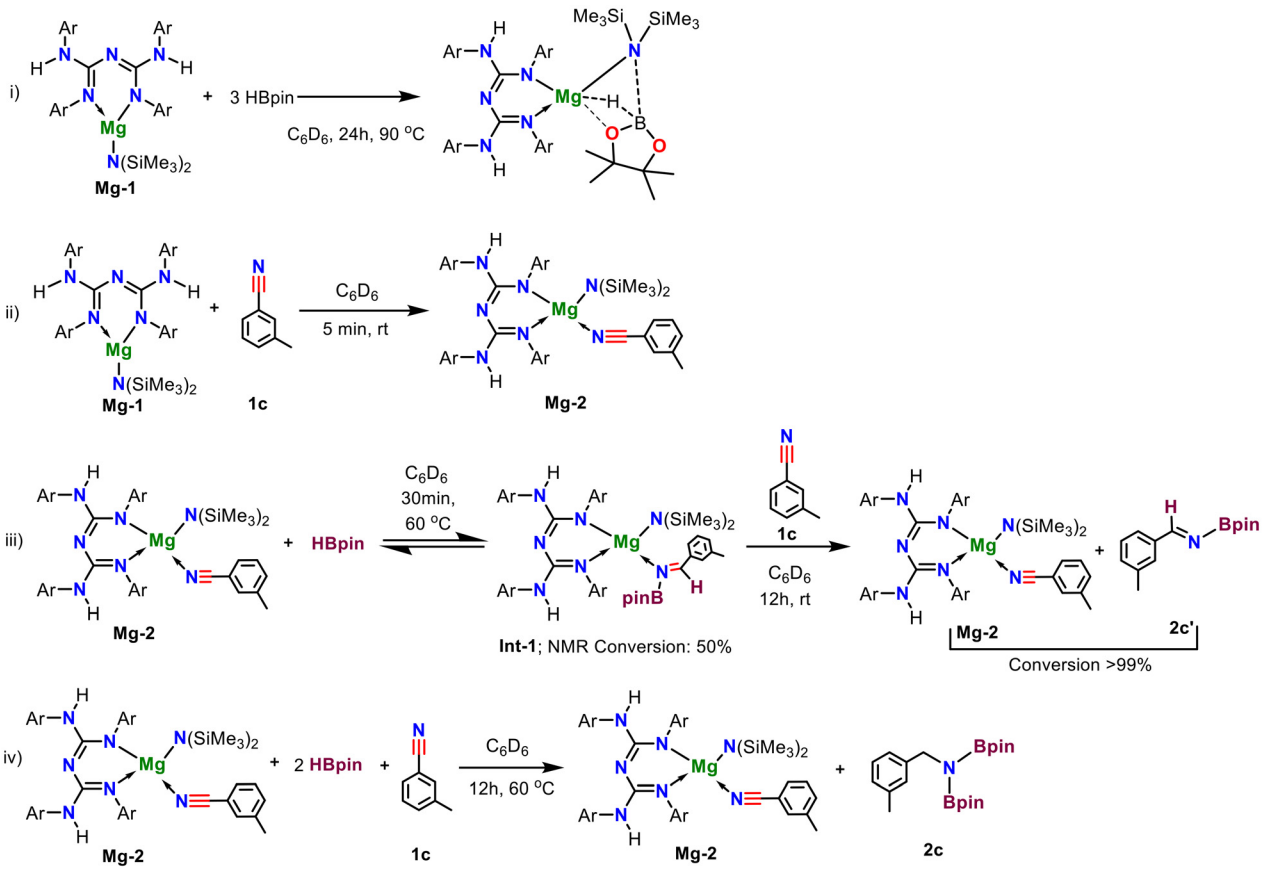

Scheme 1 Control experiments for dihydroboration of nitrile.

(CN) group, attaining a distorted tetrahedral geometry (Fig. 3). The Mg1–N6 bond distance of the compound **Mg-2** is 2.0036 (14) Å, significantly longer than the Mg–N(SiMe$_3$)$_2$ bond distance of 1.9503 (14) Å in **Mg-1**,[74] which is due to the enhanced steric hindrance at the magnesium centre in **Mg-2** than **Mg-1**.

The N atom of the nitrile is attached to the magnesium through a coordinate bond, which is evident from the longer Mg1–N7 bond distance of 2.1546 (14) Å than the purely covalent Mg1–N6 bond distance of 2.0036 (14) Å. The C3–N7 bond distance is 1.140 (2) Å, which is well in agreement with the C≡N moiety of the nitrile functional group, which confirms that the nitrile group is intact and coordinated to the magnesium centre. The N1–Mg1–N2 bite angle in the **Mg-2** is 89.64 (5)°, which is acute than the bite angle of both the bis-guanidinate [94.36 (6)°][74] as well as Nacnac stabilized amido magnesium complexes [95.11(6)°].[88]

Attempts to isolate *N*-borylimine intermediates from catalytic reactions of **1c** with HBpin were unsuccessful, likely due to their high reactivity than nitriles, leading to full reduction of *N*,*N*-bis(boryl) amine.[89,90] Notably, there have been a few reports on monohydroboration of nitriles.[44,91–96]

Surprisingly, in a 1 : 1 stoichiometric reaction of **Mg-2** and HBpin at 60 °C in C_6D_6 for 30 min, we observed the formation of an entirely new magnesium *N*-boryl imine compound **Int-1** (Scheme 1iii), where a *N*-borylated imine part is stabilized by the guanidinate magnesium amide counterpart. The **Int-1** was obtained with 50% NMR yield and was identified through ^{1}H NMR spectroscopy [see SI, Fig. S9]. A diagnostic singlet signal at 8.72 ppm in the ^{1}H NMR spectrum of **Int-1**, in C_6D_6, indicates the Mg-N(Bpin)=C–*H* moiety of the newly formed borylated imine. This is comparable to the Hill group's reported Nacnac stabilized magnesium aldimidoborohydride, where the imine N=C–H proton resonates near 9.27 ppm in the ^{1}H NMR spectrum.[57] Further heating of the reaction mixture started to produce the fully reduced *N*,*N*-bis(boryl) amine. A very careful addition of *m*-tolunitrile (**1c**) to the mixture of **Mg-2** and **Int-1**, at room temperature slowly formed the *N*-borylated imine (**2c′**) and regenerated **Mg-2**, within 12 h (Scheme 1iii) [see SI, Fig. S11] with a quantitative conversion, which implies that the **Mg-2** and **Int-1** are in equilibrium in the reaction mixture. Further isolation of the **2c′** was unsuccessful due to the extreme reactivity of the compound; it couldn't be stabilized in its imine form. Despite several attempts, we were unable to isolate the **Int-1** in its solid-state form. All the sets of stoichiometric reactions are summarized in the stacked ^{1}H NMR representation in Fig. 4.

The overall study suggests that the reaction proceeds *via* an *in situ* formation of an active magnesium hydride species by Mg–N/H–B metathesis upon treatment of HBpin with **Mg-2** (Scheme 3, *vide infra*). The formation of the adduct is a crucial

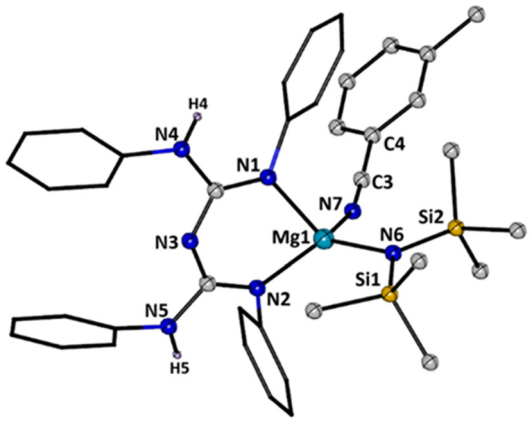

Fig. 3 Molecular structure of **Mg-2**. The thermal ellipsoids are shown at probability 50%, and H atoms except H4 and H5, and the ethyl substitutions on the *N*-aryl groups of the bis-guanidinate ligand are omitted for clarity. The selected bond lengths (Å) and bond angles (°): Mg1–N6 2.0036 (14), Mg1–N2 2.0427 (13), Mg1–N1 2.0447 (13), Mg1–N7 2.1546 (14), Si1–N6 1.7014 (13), Si2–N6 1.7039 (13), N7–C3 1.140 (2), N1–Mg1–N2 89.64 (5), N1–Mg1–N6 119.13 (6), N2–Mg1–N6 134.40 (6), Mg1–N7–C3 156.68 (14), Si1–N6–Mg1 120.66 (7), Si2–N6–Mg1 117.55 (7), Si1–N6–Si2 121.56 (8).

step, as it weakens the Mg–N($SiMe_3$)$_2$ bond [**Mg-2**; Mg1–N6: 2.0036(14) Å, Mg-1; Mg–N: 1.9503(14) Å], making it more susceptible to metathesis with HBpin. This process drives the overall reaction forward, indicating a substrate-assisted pathway.

Next, a 1 : 2 stoichiometric reaction of **Mg-2** and HBpin in the presence of *m*-tolunitrile at 60 °C in C_6D_6 formed the *N*,*N*-bis(boryl) amine **2c**, and along with the regeneration of the compound **Mg-2** (Scheme 1iv) within 12 h [see SI, Fig. S10]. The formation of the compound **2c** was confirmed by ^{1}H NMR spectroscopy. The disappearance of the singlet signal at 8.72 ppm in the ^{1}H NMR spectrum in C_6D_6 and the formation of a new signal at 4.63 ppm indicate the CH_2 protons of the N(Bpin)$_2$-CH_2-Ar moiety, which confirms the production of the compound **2c**.

A 1 : 1 stoichiometric reaction between **Mg-1** and 2,6-dimethylphenyl isocyanide (**3a**) in C_6D_6 readily formed the monomeric isocyanide adduct LMg-N($SiMe_3$)$_2$·2,6-Me_2-C_6H_3NC **Mg-3** within 5 min at room temperature (Scheme 2i).

The compound **Mg-3** was isolated and characterized by multinuclear NMR spectroscopy and single-crystal X-ray diffraction. **Mg-3** has shown a significant downfield shift of the 18H of the N($SiMe_3$)$_2$ group at 0.18 ppm (**Mg-1**; N($SiMe_3$)$_2$: δ 0.01 ppm) in the ^{1}H NMR spectrum in C_6D_6, indicating the coordination of the electron-withdrawing N═C group. A singlet signal at 2.00 ppm, in the ^{1}H NMR spectrum, corresponding to the methyl groups of the 2,6-dimethylphenyl isocyanide. Additionally, the ^{29}Si{^{1}H} NMR spectrum displays a singlet signal at −7.69 ppm in C_6D_6, significantly shifted from

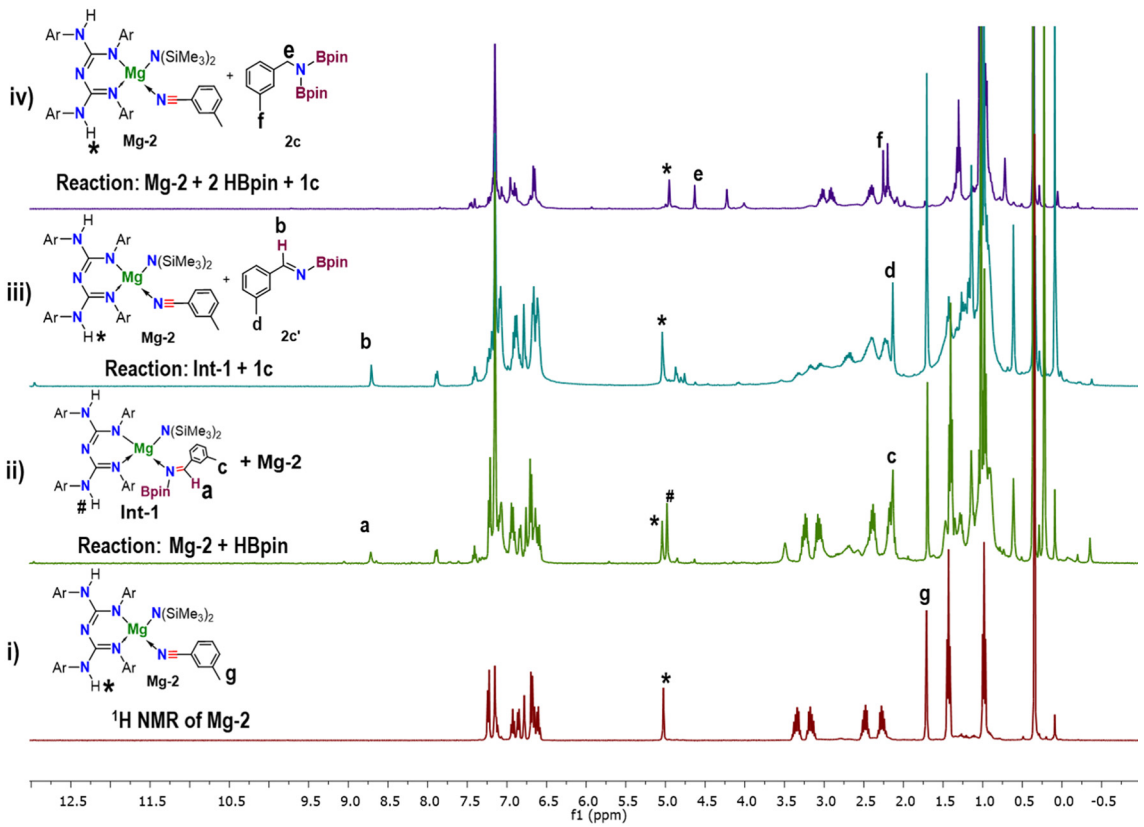

Fig. 4 Stacked ^{1}H NMR spectra for the stoichiometric reactions.

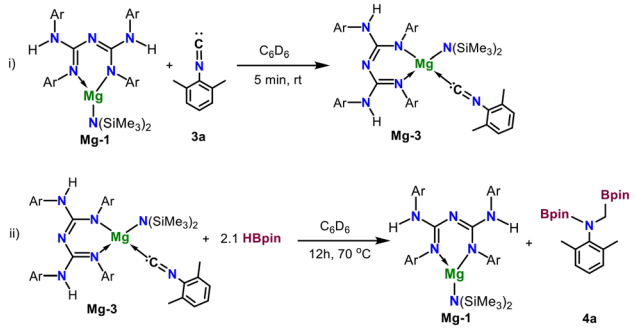

Scheme 2 Control experiments for dihydroboration of isocyanide.

its parent precursor **Mg-1** at −7.22 ppm, confirming the formation of the **Mg-3** [see SI, Fig. S4–S6]. Diffractable single crystals of the compound **Mg-3** were grown inside the J. Young valve NMR tube at room temperature in C_6D_6. The X-ray analysis shows the compound **Mg-3** crystallizes in a monoclinic system with a P-1 space group. The molecular structure displayed a monomeric structure where one molecule of 2,6-dimethylphenyl isocyanide is coordinated to the magnesium centre of **Mg-1**, through the carbon atom, making it a four-coordinated magnesium complex with a distorted tetrahedral geometry (Fig. 5). To the best of our knowledge, **Mg-3** is the first example of an isocyanide adduct of a bis-guanidinate magnesium complex. The Mg1–N6 bond distance is 2.0077 (13) Å, significantly longer than the parent precursor **Mg-1** (Mg-N($SiMe_3$)$_2$; 1.9503 (14) Å), corresponding to the enhanced

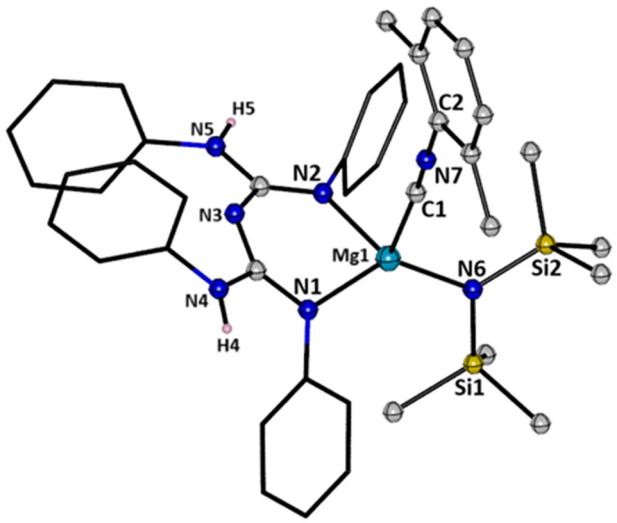

Fig. 5 Molecular structure of compound **Mg-3**. The thermal ellipsoids are shown at probability 50%, and H atoms except H4 and H5 and the ethyl substitutions on the *N*-aryl groups of the bis-guanidinate ligand are omitted for clarity. The selected bond lengths (Å) and bond angles (°): Mg1–N6 2.0077 (13), Mg1–N2 2.0492 (12), Mg1–N1 2.0681 (12), Mg1–C1 2.3599 (16), Si1–N6 1.7067 (13), Si2–N6 1.7132 (13), N7–C1 1.159 (2), N1–Mg1–N2 90.53 (5), N1–Mg1–N6 132.50 (5), N2–Mg1–N6 120.99 (5), Mg1–C1–N1 176.39 (12), Si1–N6–Mg1 120.17 (7), Si2–N6–Mg1 120.89 (7), Si1–N6–Si2 118.88 (7).

steric hindrance due to the increased coordination number to the magnesium centre. The C1–N7 bond distance in the coordinated isocyanide counterpart is 1.159 (2) Å, slightly longer than the C–N bond distance [N3–C38 1.145 (3) Å] in the isocyanide adduct of the analogous Nacnac stabilized magnesium siloxide,[97] reported by Hill and coworkers. The C1–N7–C2 bond angle is 178.53 (16)°, which implies a close to linear framework of the isocyanide moiety. The longer C1–N7 bond distance indicates the ease of the B–H addition to the isocyanide R–N═C: bond. Similar to the **Mg-2**, the N1–Mg1–N2 bite angle in the compound **Mg-3** is 90.53 (5)°, which is acute than the bite angles of both the **Mg-1**[74] as well as the analogous Nacnac magnesium amide complex (*vide supra*).[88]

A subsequent stoichiometric reaction of compound **Mg-3** with 2 equiv. of HBpin at 70 °C for 12 h formed the *N*,*C*-di(boryl)amine **4a** and **Mg-1** with a quantitative conversion (Scheme 2ii), verified through ^{1}H NMR spectroscopy [see SI, Fig. S12].

Kinetic experiments and discussions

To justify the mechanistic implications of the stoichiometric outcomes, a kinetic study *via* comparison of concentration profiles[98] for the **Mg-1**-catalyzed nitrile's dihydroboration was conducted. The *m*-tolunitrile(**1c**) was chosen as a standard substrate because of its indicative signals for its consumption and the formation of the product in the ^{1}H NMR spectrum. All the reactions were carried out at 343 K and were monitored by ^{1}H NMR spectroscopy up to 80% conversion with respect to mesitylene used as an internal standard, using 10 mol% of the **Mg-1** with various ratios of *m*-tolunitrile to HBpin.

A 1 : 2 stoichiometric ratio of *m*-tolunitrile (**1c**) (0.16 M) and HBpin (0.33 M), with varying catalyst load of **Mg-1** adjusted at 10 and 7 mol%, apparently displayed a first order kinetics, (Fig. 6A) consistent with other Nacnac stabilized alkaline earth metal complexes mediated catalysis reactions.[57,99–101] This observation indicates involvement of a single isolated magnesium center, which is involved in the rate determination of the reaction.

A series of pseudo-first-order reactions was conducted using a 20-fold excess of *m*-tolunitrile (3.33 M) and a catalyst loading of 0.0167 M while varying HBpin concentrations from 0.33 M to 1.33 M. The reaction rate displayed a clear first-order kinetics at lower HBpin concentrations (0.33 M and 0.66 M) but deviated to a near-zero-order dependence at higher concentrations (1.00 M, 1.16 M, and 1.33 M) (Fig. 6B). It was observed that the rate of product formation increased significantly from 0.33 M to 0.66 M HBpin, whereas only a marginal change was observed between 1.00 M and 1.33 M, indicating saturation kinetics, consistent with the formation of a catalyst–substrate intermediate species (designated as **Int-1**) similar to the Hill group's reported magnesium-catalyzed nitriles dihydroboration.[57] This saturation behavior suggests a Michaelis–Menten–type[102,103] kinetic profile, where the reaction of **Mg-2** and HBpin proceeds through the formation of an active catalyst–HBpin intermediate (*ca.* **Int-1**), which precedes the rate-determining step.

$$\text{Catalyst} + \text{HBpin} \rightleftharpoons [\text{Catalyst-HBpin}] \rightarrow \text{Product}$$

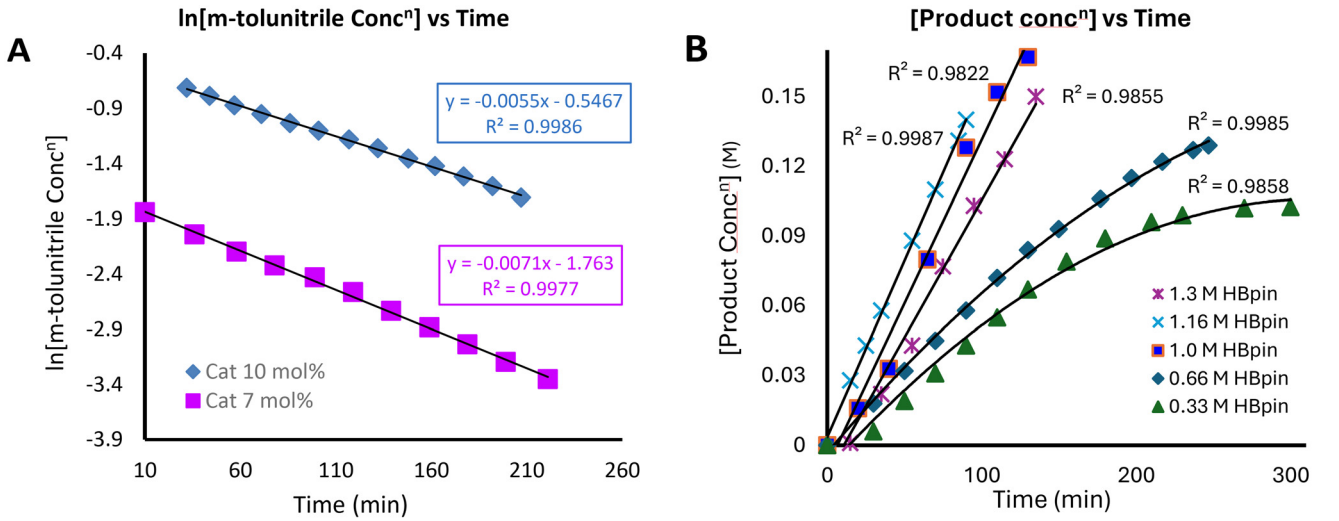

Fig. 6 (A) ln[*m*-tolunitrileConc^n] *vs.* Time plot, at different loadings of **Mg-1**. (B) [Product Conc^n] *vs.* Time plot, at pseudo-first order condition with respect to *m*-tolunitrile.

At lower concentrations of HBpin (0.33 M, 0.67 M), the active catalyst **Mg-2** remains unsaturated, and the rate increases proportionally with HBpin concentration, indicating a first-order kinetics arising from the rate-limiting formation of **Int-1**; however, at higher concentrations of HBpin (1.00 M to 1.33 M), catalyst saturation occurs, and the rate becomes independent of the concentration of HBpin, showing zero-order kinetics. This transition highlights the key role of catalyst–substrate complexation in governing the observed rate behavior. A stacked ^{1}H NMR study (Fig. 7) of the reaction pseudo-first-order conditions with respect to nitrile (20 equiv.) revealed the formation of an *N*-boryl imine intermediate (**2c′**) at high nitrile concentrations. This observation aligns with outcomes from stoichiometric reactions. As the reaction proceeds and nitrile is consumed, **2c′** formation drops while the final product **2c** starts to appear. The **2c′** is observed only under stoichiometric and kinetic conditions, not in catalytic runs, suggesting it is a short-lived intermediate.

To investigate the effect of nitrile concentration on the reaction rate, a series of catalytic reactions was conducted using 0.0167 M **Mg-1** under pseudo-first-order conditions with respect to HBpin (3.33 M, 20-fold excess), while varying the concentration of *m*-tolunitrile (0.167–0.67 M).

At lower nitrile concentrations (0.167 and 0.33 M), a zero-order kinetics was observed, indicating that nitrile's concentration plays no direct role in the rate-determining step and is

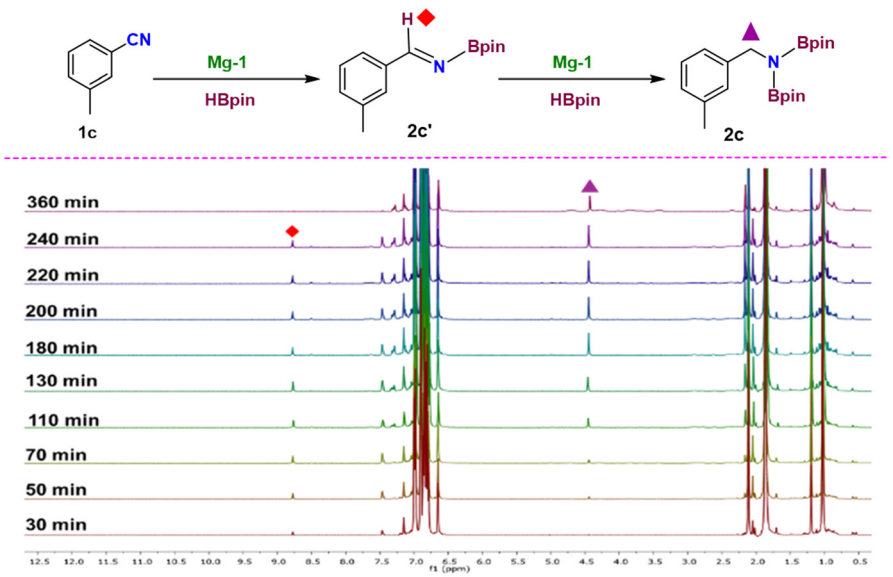

Fig. 7 Stacked ^{1}H NMR spectra (400 MHz) for the reaction of *m*-tolunitrile (**1c**) (3.33 M, 20 equiv.), HBpin (0.33 M, 2 equiv.), and **Mg-1** (10 mol%, 0.0167 M) in C_6D_6. Spectra were recorded at 70 °C, in different time intervals from 30 min to 360 min. **2c′**; ♦ 3-CH_3-C_6H_4-CH=N(Bpin). **2c**; ▲ 3-CH_3-C_6H_4-C**H2**-N(Bpin)$_2$.

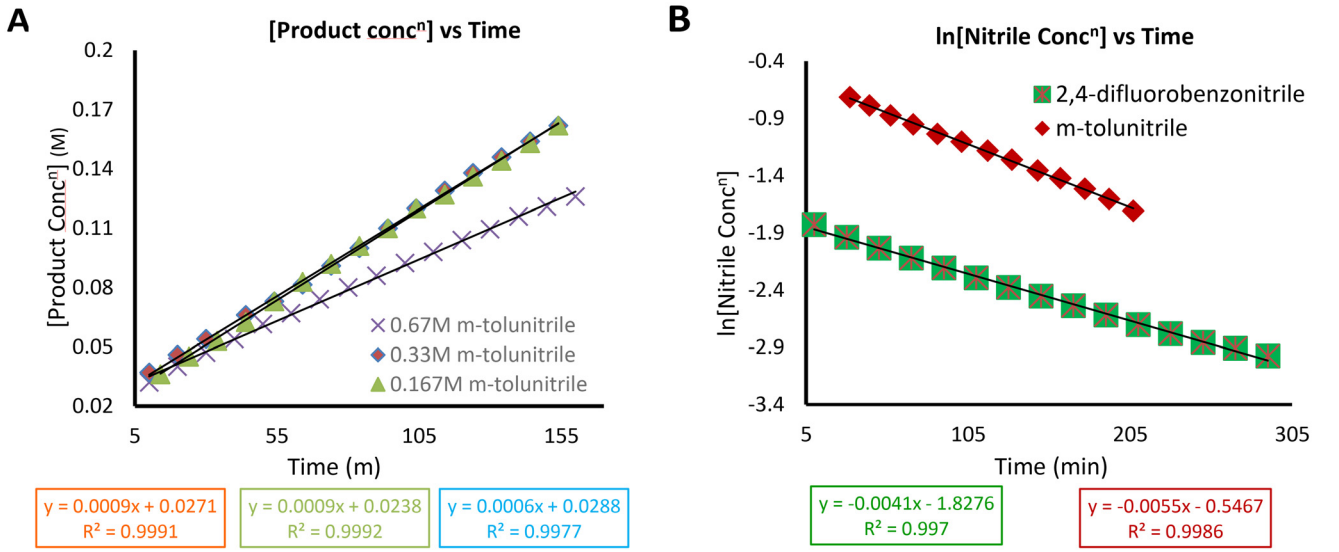

Fig. 8 (A) [Product Conc^n] *vs.* time plot, at pseudo-first order condition with respect to HBpin, linear fit. (B) ln[Nitrile Conc^n] *vs.* Time plot, for electron withdrawing and electron donating substituted aryl nitriles, linear fit.

only involved in the formation of the catalytically active species, **Mg-2**. However, at higher nitrile concentration (0.67 M), the reaction rate decreased despite maintaining a zero-order kinetics, suggesting that excess nitrile concentration inhibits the reaction by saturation of the **Mg-2** active site and impeding HBpin access (Fig. 8A).

A further study examined the effect of electron-donating and electron-withdrawing groups on the reaction mechanism (Fig. 8B). The dihydroboration of 2,4-difluorobenzonitrile (**1i**) proceeded with a slightly decreased rate with respect to *m*-tolunitrile (**1c**), following first-order kinetics. The slightly reduced reaction rate for **1i** is likely due to its strong electron-withdrawing nature and more steric hindrance, which decreases the availability of the nitrile lone pair for coordination with **Mg-1**. This in turn, inhibits the formation of [**Mg-1** nitrile] adduct, a key step in the overall reaction pathway. Further study of dihydroboration of both the electron-withdrawing (**1m**) and the electron-donating (**1c**) substituted nitriles within initial 3 h, exhibited nearly similar reaction rate, highlighting the importance of the formation [**Mg-1** nitrile] adduct.

In summary, kinetic studies show that the reaction follows first-order kinetics with respect to the magnesium catalyst, indicating the involvement of a single active species governing the reaction rate. Nitriles exhibit zero-order kinetics; however, they inhibit the reaction rate at higher concentrations due to catalyst saturation. HBpin shows first-order kinetics at low concentrations, shifting to zero-order at higher concentrations, consistent with the formation of a catalyst–substrate intermediate, indicating a Michaelis–Menten-type behavior. Electron-withdrawing nitriles, such as 2,4-difluorobenzonitrile, suppress the reaction rate slightly by weakening coordination to the magnesium center. Overall, the catalytic cycle is primarily governed by the formation of **Mg-2**, and its reaction with HBpin.

The rate of the reaction follows eqn (1) and (2).
(At a lower concentration of HBpin)

$$\frac{\partial p}{\partial t} = k_{obs} \cdot [\mathbf{Mg-1}]^1 \cdot [\text{Nitrile}]^0 \cdot [\text{HBpin}]^1 \quad (1)$$

(At a higher concentration of HBpin)

$$\frac{\partial p}{\partial t} = k_{obs} \cdot [\mathbf{Mg-1}]^1 \cdot [\text{Nitrile}]^0 \cdot [\text{HBpin}]^0 \quad (2)$$

Catalytic cycle for the dihydroboration of nitriles

Based on stoichiometric reactions and the previous literature reports,[38,104] we propose a (Scheme 3) a plausible mechanistic cycle for the **Mg-1**-catalyzed hydroboration of organic nitriles and isocyanides. As far as magnesium-catalyzed hydroboration is concerned, initially **Mg-1** reacts with nitrile **1c** to form the active species bis-guanidinate magnesium nitrile adduct **Mg-2**. The reaction of **Mg-2** and HBpin, generates a short-lived magnesium imido intermediate **Int-1′** *via in situ* hydride formation. This species subsequently undergoes rapid reaction with pinB-N($SiMe_3$)$_2$ (Scheme 3) to afford magnesium amino-*N*-boryl imine intermediate (**Int-1**). The **Int-1** simultaneously reacts with HBpin to form **Int-2**, which, upon reacting with *m*-tolunitrile (**1c**), produces the desired *N*,*N*′-bis-boryl amine (**2c**) and regenerates the active species **Mg-2**, hereby closing the catalytic cycle. Notably, at the outset, **Int-1** remains in equilibrium with **Mg-2**, which, upon reacting with excess *m*-tolunitrile(**1c**), possibly produces *N*-boryl imine **2c′** along with reformation of **Mg-2**; however, this has not been observed in the catalytic reactions under optimal conditions. Unlike magnesium-catalyzed dihydroboration of nitriles, **Mg-1** acts as an active catalyst for the dihydroboration of isocyanides. Initially, the **Mg-1** reacts with **3a** and forms intermediate **Mg-3** *via* coordination of isocyanide to the magnesium

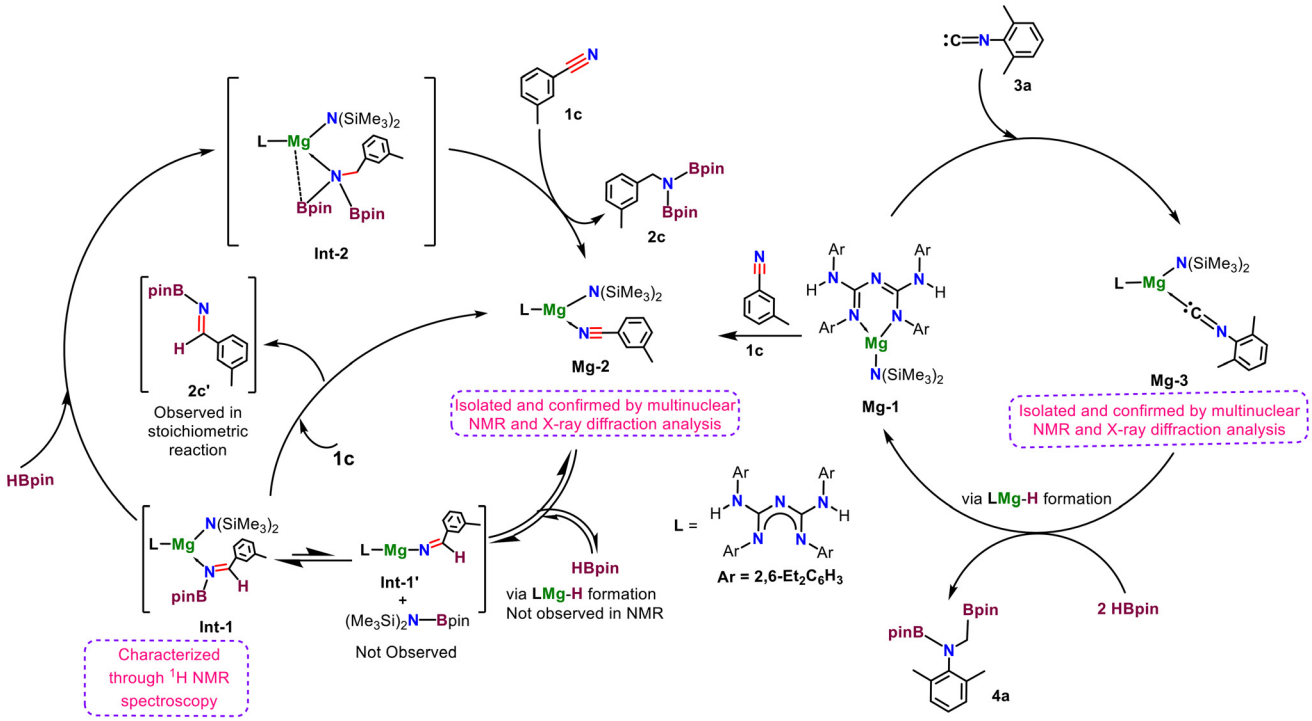

Scheme 3 Mechanistic cycle of the Mg-1-catalyzed dihydroboration of nitrile and isocyanide.

centre, which reacts with 2 equiv. of HBpin to produce the 1,2-diborylated amine **4a**, along with the regeneration of the active catalyst **Mg-1**, thereby closing the catalytic cycle (Scheme 3). The overall outcomes successfully established **Mg-1** as a pre-catalyst for the nitriles dihydroboration; however, it acts as an active catalyst for the dihydroboration of isocyanides.

Conclusion

In conclusion, we have successfully synthesized the first heteroleptic bis-guanidinate magnesium amide adducts bearing coordinated nitrile and isocyanide groups. Furthermore, we have demonstrated the magnesium amide-catalyzed hydroboration of nitriles and isocyanides *via* a substrate-assisted pathway. This catalytic protocol enables the formation of *N*,*N*-bis(boryl)amines and *N*,*C*-di(boryl)amines in good to excellent yields. Notably, we observed that in contrast to the homoleptic magnesium bis-amide, the heteroleptic *N*,*N*′-chelated bis-guanidinate magnesium amide acts as a superior catalyst for both the dihydroboration of nitriles and isocyanides. Comprehensive mechanistic investigations were established through various stoichiometric reactions, which led to the successful isolation of catalytically relevant intermediates and the active magnesium species, which were unambiguously identified using multinuclear NMR spectroscopy and single-crystal X-ray diffraction analysis. Notably, we were able to generate a highly reactive *N*-boryl imine intermediate in a stoichiometric reaction. These findings not only expand the scope of magnesium catalysis in bond-forming transformations but also provide critical mechanistic insights into substrate-assisted activation pathways in main-group catalysis.

Author contributions

S. M. carried out most of the synthesis and characterization, drafted the manuscript, and contributed to its subsequent and final versions. S. R. P. managed the supplementary data and assisted in catalyst preparation and kinetic studies. A. D. conducted the catalysis studies and contributed to manuscript drafting. S. N. conceptualized the project, acquired funding, supervised the work, and contributed to the final manuscript.

Conflicts of interest

The authors declare no conflict of interest.

Data availability

Supplementary information (SI): all the materials and instrumentation, and supplementary figures and tables. See DOI: **https://doi.org/10.1039/d5qo01184a**.

CCDC 2476567 and 2476571 contain the supplementary crystallographic data for this paper.[105a,b]

Acknowledgements

The authors thank the National Institute of Science Education and Research (NISER), Bhubaneswar, Odisha, Homi Bhabha National Institute (HBNI), Mumbai, Department of Atomic Energy (DAE), Govt. of India. The Science and Engineering Research Board (SERB), India (CRG/2021/007000) is acknowledged for providing financial support.

References

1 D. Hayrapetyan and A. Y. Khalimon, Catalytic Nitrile Hydroboration: A Route to *N*,*N*-Diborylamines and Uses Thereof, *Chem. – Asian J.*, 2020, **15**, 2575–2587.
2 P. Patil, M. Ahmadian-Moghaddam and A. Dömling, Isocyanide 2.0, *Green Chem.*, 2020, **22**, 6902–6911.
3 B. R. Barnett, C. E. Moore, A. L. Rheingold and J. S. Figueroa, Frustrated Lewis pair behavior of monomeric (boryl) iminomethanes accessed from isocyanide 1, 1-hydroboration, *Chem. Commun.*, 2015, **51**, 541–544.
4 J. S. Carey, D. Laffan, C. Thomson and M. T. Williams, Analysis of the reactions used for the preparation of drug candidate molecules, *Org. Biomol. Chem.*, 2006, **4**, 2337–2347.
5 G. P. Chiusoli and P. M. Maitlis, *Metal-catalysis in industrial organic processes*, Royal Society of Chemistry, 2019.
6 K. Hayes, Industrial processes for manufacturing amines, *Appl. Catal., A*, 2001, **221**, 187–195.
7 J. Magano and J. R. Dunetz, Large-Scale Applications of Transition Metal-Catalyzed Couplings for the Synthesis of Pharmaceuticals, *Chem. Rev.*, 2011, **111**, 2177–2250.
8 R. Martin and S. L. Buchwald, Palladium-catalyzed Suzuki–Miyaura cross-coupling reactions employing dialkylbiaryl phosphine ligands, *Acc. Chem. Res.*, 2008, **41**, 1461–1473.
9 T. Renders, S. Van de Vyver and B. F. Sels, Bio-based amines through sustainable heterogeneous catalysis, *Green Chem.*, 2017, **19**, 5303–5331.
10 C. Torborg and M. Beller, Catalysis, Recent applications of palladium–catalyzed coupling reactions in the pharmaceutical, agrochemical, and fine chemical industries, *Adv. Synth. Catal.*, 2009, **351**, 3027–3043.
11 N. Miyaura and A. Suzuki, Palladium-Catalyzed Cross-Coupling Reactions of Organoboron Compounds, *Chem. Rev.*, 1995, **95**, 2457–2483.
12 C. Pubill-Ulldemolins, A. Bonet, C. Bo, H. Gulyás and E. Fernández, A new context for palladium mediated B-addition reaction: an open door to consecutive functionalization, *Org. Biomol. Chem.*, 2010, **8**, 2667–2682.
13 C. C. Chong and R. Kinjo, Catalytic Hydroboration of Carbonyl Derivatives, Imines, and Carbon Dioxide, *ACS Catal.*, 2015, **5**, 3238–3259.
14 M. M. Roy, A. A. Omana, A. S. Wilson, M. S. Hill, S. Aldridge and E. Rivard, Molecular main group metal hydrides, *Chem. Rev.*, 2021, **121**, 12784–12965.
15 Q. Wang, J. Guo and P. Chen, Complex transition metal hydrides for heterogeneous catalysis, *Chem. Catal.*, 2023, **3**, 100524.
16 N. Klopčič, I. Grimmer, F. Winkler, M. Sartory and A. Trattner, A review on metal hydride materials for hydrogen storage, *J. Energy Storage*, 2023, **72**, 108456.
17 J. G. de Vries and C. J. Elsevier, *Handbook of homogeneous hydrogenation*, Weinheim: Wiley-VCH, 2007.
18 P. Andersson, *Modern Reduction Methods*, Wiley-VCH, 2008.
19 K. Kuciński and G. Hreczycho, Hydrosilylation and hydroboration in a sustainable manner: from Earth-abundant catalysts to catalyst-free solutions, *Green Chem.*, 2020, **22**, 5210–5224.
20 M. L. Shegavi and S. K. Bose, Recent advances in the catalytic hydroboration of carbonyl compounds, *Catal. Sci. Technol.*, 2019, **9**, 3307–3336.
21 M. Magre, M. Szewczyk and M. Rueping, s-Block Metal Catalysts for the Hydroboration of Unsaturated Bonds, *Chem. Rev.*, 2022, **122**, 8261–8312.
22 S. J. Geier, C. M. Vogels, J. A. Melanson and S. A. Westcott, The transition metal-catalysed hydroboration reaction, *Chem. Soc. Rev.*, 2022, **51**, 8877–8922.
23 C. Jensen, The advantages and difficulties of recent work in molecular catalysis, *J. Thermodyn. Catal.*, 2022, **13**, 1–2.
24 S. K. Bose, L. Mao, L. Kuehn, U. Radius, J. Nekvinda, W. L. Santos, S. A. Westcott, P. G. Steel and T. B. Marder, First-Row d-Block Element-Catalyzed Carbon–Boron Bond Formation and Related Processes, *Chem. Rev.*, 2021, **121**, 13238–13341.
25 M. Rauch, S. Ruccolo and G. Parkin, Synthesis, Structure, and Reactivity of a Terminal Magnesium Hydride Compound with a Carbatrane Motif, [TismPriBenz]MgH: A Multifunctional Catalyst for Hydrosilylation and Hydroboration, *J. Am. Chem. Soc.*, 2017, **139**, 13264–13267.
26 D. Shakhman, A. Dmitrienko, M. Pilkington and G. I. Nikonov, Selective Zinc-Catalyzed 1,2-hydroboration of N-heteroaromatics via a Non–Hydride Mechanism, *Eur. J. Inorg. Chem.*, 2023, **26**, e202300293.
27 D. Mukherjee, S. Shirase, T. P. Spaniol, K. Mashima and J. Okuda, Magnesium hydridotriphenylborate [$Mg(thf)_6$][$HBPh_3$]$_2$: a versatile hydroboration catalyst, *Chem. Commun.*, 2016, **52**, 13155–13158.
28 C. Ginés, B. Parra-Cadenas, R. Fernández-Galán, D. García-Vivó, D. Elorriaga, A. Ramos and F. Carrillo-Hermosilla, Magnesium and Calcium Bisguanidinates: Catalytic Activity in the Hydroboration of Unsaturated Molecules, *Adv. Synth. Catal.*, 2025, **367**, e202400843.
29 S. Ataie and R. T. Baker, Comparing B–H Bond Activation in NiIIX(NNN)-Catalyzed Nitrile Dihydroboration (X = Anionic N-, C-, O-, S-, or P-donor), *Inorg. Chem.*, 2022, **61**, 19998–20007.
30 J. C. Babón, M. A. Esteruelas, I. Fernández, A. M. López and E. Oñate, Dihydroboration of Alkyl Nitriles Catalyzed by an Osmium-Polyhydride: Scope, Kinetics, and Mechanism, *Organometallics*, 2020, **39**, 3864–3872.

31 I. Banerjee, S. Anga, K. Bano and T. K. Panda, Efficient and chemoselective hydroboration of organic nitriles promoted by TiIV catalyst supported by unsymmetrical acenaphthenequinonediimine ligand, *J. Organomet. Chem.*, 2019, **902**, 120958.
32 A. R. Bazkiaei, M. Wiseman and M. Findlater, Iron-catalysed hydroboration of non-activated imines and nitriles: kinetic and mechanistic studies, *RSC Adv.*, 2021, **11**, 15284–15289.
33 H. Ben-Daat, C. L. Rock, M. Flores, T. L. Groy, A. C. Bowman and R. J. Trovitch, Hydroboration of alkynes and nitriles using an α-diimine cobalt hydride catalyst, *Chem. Commun.*, 2017, **53**, 7333–7336.
34 J. Bhattacharjee, A. Harinath, K. Bano and T. K. Panda, Highly Chemoselective Hydroboration of Alkynes and Nitriles Catalyzed by Group 4 Metal Amidophosphine–Borane Complexes, *ACS Omega*, 2020, **5**, 1595–1606.
35 S. Caddick, D. B. Judd, A. K. d. K. Lewis, M. T. Reich and M. R. V. Williams, A generic approach for the catalytic reduction of nitriles, *Tetrahedron*, 2003, **59**, 5417–5423.
36 S. Das, J. Maity and T. K. Panda, Metal/Non-Metal Catalyzed Activation of Organic Nitriles, *Chem. Rec.*, 2022, **22**, e202200192.
37 J. B. Geri and N. K. Szymczak, A Proton-Switchable Bifunctional Ruthenium Complex That Catalyzes Nitrile Hydroboration, *J. Am. Chem. Soc.*, 2015, **137**, 12808–12814.
38 C. Ghosh, S. Kim, M. R. Mena, J.-H. Kim, R. Pal, C. L. Rock, T. L. Groy, M.-H. Baik and R. J. Trovitch, Efficient Cobalt Catalyst for Ambient-Temperature Nitrile Dihydroboration, the Elucidation of a Chelate-Assisted Borylation Mechanism, and a New Synthetic Route to Amides, *J. Am. Chem. Soc.*, 2019, **141**, 15327–15337.
39 K. A. Gudun, A. Slamova, D. Hayrapetyan and A. Y. Khalimon, Efficient Co-Catalyzed Double Hydroboration of Nitriles: Application to One-Pot Conversion of Nitriles to Aldimines, *Chem. – Eur. J.*, 2020, **26**, 4963–4968.
40 A. D. Ibrahim, S. W. Entsminger and A. R. Fout, Insights into a Chemoselective Cobalt Catalyst for the Hydroboration of Alkenes and Nitriles, *ACS Catal.*, 2017, **7**, 3730–3734.
41 M. Itazaki and H. Nakazawa, Selective Double Addition Reaction of an E-H Bond (E = Si, B) to a C≡N Triple Bond of Organonitriles, *Molecules*, 2018, **23**, 2769.
42 A. Kaithal, B. Chatterjee and C. Gunanathan, Ruthenium-Catalyzed Selective Hydroboration of Nitriles and Imines, *J. Org. Chem.*, 2016, **81**, 11153–11161.
43 A. Y. Khalimon, P. Farha, L. G. Kuzmina and G. I. Nikonov, Catalytic hydroboration by an imido-hydrido complex of Mo(iv), *Chem. Commun.*, 2012, **48**, 455–457.
44 T. Kitano, T. Komuro and H. Tobita, Double and Single Hydroboration of Nitriles Catalyzed by a Ruthenium–Bis (silyl)xanthene Complex: Application to One-Pot Synthesis of Diarylamines and N-Arylimines, *Organometallics*, 2019, **38**, 1417–1420.
45 G. Nakamura, Y. Nakajima, K. Matsumoto, V. Srinivas and S. Shimada, Nitrile hydroboration reactions catalysed by simple nickel salts, bis(acetylacetonato)nickel(II) and its derivatives, *Catal. Sci. Technol.*, 2017, **7**, 3196–3199.
46 T. T. Nguyen, J.-H. Kim, S. Kim, C. Oh, M. Flores, T. L. Groy, M.-H. Baik and R. J. Trovitch, Scope and mechanism of nitrile dihydroboration mediated by a β-diketiminate manganese hydride catalyst, *Chem. Commun.*, 2020, **56**, 3959–3962.
47 V. K. Pandey, C. S. Tiwari and A. Rit, Silver-Catalyzed Hydroboration of C–X (X = C, O, N) Multiple Bonds, *Org. Lett.*, 2021, **23**, 1681–1686.
48 Z. Huang, S. Wang, X. Zhu, Q. Yuan, Y. Wei, S. Zhou and X. Mu, Well-Defined Amidate-Functionalized N-Heterocyclic Carbene -Supported Rare-Earth Metal Complexes as Catalysts for Efficient Hydroboration of Unactivated Imines and Nitriles, *Inorg. Chem.*, 2018, **57**, 15069–15078.
49 S. Pradhan, R. V. Sankar and C. Gunanathan, A Boron-Nitrogen Double Transborylation Strategy for Borane-Catalyzed Hydroboration of Nitriles, *J. Org. Chem.*, 2022, **87**, 12386–12396.
50 B. Yan, X. He, C. Ni, Z. Yang and X. Ma, *n*-Butyllithium Catalyzed Hydroboration of Nitriles and Carbodiimides, *ChemCatChem*, 2021, **13**, 851–854.
51 P. Ghosh and A. J. von Wangelin, Lithium amide catalyzed hydroboration of nitriles, *Org. Chem. Front.*, 2020, **7**, 960–966.
52 D. Bedi, A. Brar and M. Findlater, Transition metal- and solvent-free double hydroboration of nitriles, *Green Chem.*, 2020, **22**, 1125–1128.
53 W. Liu, Y. Ding, D. Jin, Q. Shen, B. Yan, X. Ma and Z. Yang, Organic aluminum hydrides catalyze nitrile hydroboration, *Green Chem.*, 2019, **21**, 3812–3815.
54 A. Harinath, J. Bhattacharjee and T. K. Panda, Catalytic Hydroboration of Organic Nitriles Promoted by Aluminum Complex, *Adv. Synth. Catal.*, 2019, **361**, 850–857.
55 Y. Ding, X. Ma, Y. Liu, W. Liu, Z. Yang and H. W. Roesky, Alkylaluminum Complexes as Precatalysts in Hydroboration of Nitriles and Carbodiimides, *Organometallics*, 2019, **38**, 3092–3097.
56 J. Li, M. Luo, X. Sheng, H. Hua, W. Yao, S. A. Pullarkat, L. Xu and M. Ma, Unsymmetrical β-diketiminate magnesium(I) complexes: syntheses and application in catalytic hydroboration of alkyne, nitrile and carbonyl compounds, *Org. Chem. Front.*, 2018, **5**, 3538–3547.
57 C. Weetman, M. D. Anker, M. Arrowsmith, G. Kociok-Köhn, D. J. Liptrot, M. F. Mahon and M. S. Hill, Magnesium-catalysed nitrile hydroboration, *Chem. Sci.*, 2016, **7**, 628–641.
58 M. Arrowsmith, M. S. Hill and G. Kociok-Köhn, Magnesium Catalysis of Imine Hydroboration, *Chem. – Eur. J.*, 2013, **19**, 2776–2783.
59 D. Haddenham, L. Pasumansky, J. DeSoto, S. Eagon and B. Singaram, Reductions of Aliphatic and Aromatic

Nitriles to Primary Amines with Diisopropylaminoborane, *J. Org. Chem.*, 2009, **74**, 1964–1970.
60 X. Wang and X. Xu, Hydroboration of nitriles and imines by highly active zinc dihydride catalysts, *RSC Adv.*, 2021, **11**, 1128–1133.
61 S. Das, J. Bhattacharjee and T. K. Panda, An imidazolin-2-iminato ligand organozinc complex as a catalyst for hydroboration of organic nitriles, *New J. Chem.*, 2019, **43**, 16812–16818.
62 N. Sarkar, S. Bera and S. Nembenna, Aluminum-Catalyzed Selective Hydroboration of Nitriles and Alkynes: A Multifunctional Catalyst, *J. Org. Chem.*, 2020, **85**, 4999–5009.
63 C. Weetman, M. S. Hill and M. F. Mahon, Magnesium-catalysed hydroboration of isonitriles, *Chem. Commun.*, 2015, **51**, 14477–14480.
64 R. K. Sahoo, S. Rajput, S. Dutta, K. Sahu and S. Nembenna, Zinc Hydride-Catalyzed Dihydroboration of Isonitriles and Nitriles: Mechanistic Studies with the Structurally Characterized Zinc Intermediates, *Organometallics*, 2023, **42**, 2293–2303.
65 S. Ataie, J. S. Ovens and R. T. Baker, Solvent-free Zn (NSNO) complex-catalysed dihydroboration of nitriles, *Chem. Commun.*, 2022, **58**, 8266–8269.
66 S. Saha and M. S. Eisen, Catalytic Recycling of a Th–H Bond via Single or Double Hydroboration of Inactivated Imines or Nitriles, *ACS Catal.*, 2019, **9**, 5947–5956.
67 Y. Sarazin and P. M. Chapple, in *Comprehensive Organometallic Chemistry IV*, ed. G. Parkin, K. Meyer and D. O'hare, Elsevier, Oxford, 2022, pp. 104–192.
68 S. Nembenna, N. Sarkar, R. K. Sahoo and S. Mukhopadhyay, in *Comprehensive Organometallic Chemistry IV*, ed. G. Parkin, K. Meyer and D. O'hare, Elsevier, Oxford, 2022, pp. 71–241.
69 M. S. Hill, D. J. Liptrot and C. Weetman, Alkaline earths as main group reagents in molecular catalysis, *Chem. Soc. Rev.*, 2016, **45**, 972–988.
70 M. R. Crimmin and M. S. Hill, in *Alkaline-Earth Metal Compounds: Oddities and Applications*, ed. S. Harder, Springer Berlin Heidelberg, Berlin, Heidelberg, 2013, pp. 191–241.
71 S. Harder, From Limestone to Catalysis: Application of Calcium Compounds as Homogeneous Catalysts, *Chem. Rev.*, 2010, **110**, 3852–3876.
72 A. Stasch, in *Catalysis with Earth-abundant Elements*, ed. U. Schneider and S. Thomas, The Royal Society of Chemistry, 2020, pp. 55–80. DOI: **10.1039/9781788012775-00055**.
73 M. J. Evans and C. Jones, Low oxidation state and hydrido group 2 complexes: synthesis and applications in the activation of gaseous substrates, *Chem. Soc. Rev.*, 2024, **53**, 5054–5082.
74 S. Mukhopadhyay, S. Rajput, R. K. Sahoo and S. Nembenna, Insights Into the Magnesium-Catalyzed C–C Coupling of Terminal Alkynes with Carbodiimides, *Eur. J. Org. Chem.*, 2024, e202400702.
75 T. Peddarao, A. Baishya, N. Sarkar, R. Acharya and S. Nembenna, Conjugated Bis-Guanidines (CBGs) as β-Diketimine Analogues: Synthesis, Characterization of CBGs/Their Lithium Salts and CBG Li Catalyzed Addition of B–H and TMSCN to Carbonyls, *Eur. J. Inorg. Chem.*, 2021, **2021**, 2034–2046.
76 R. K. Sahoo, N. Sarkar and S. Nembenna, Zinc Hydride Catalyzed Chemoselective Hydroboration of Isocyanates: Amide Bond Formation and C=O Bond Cleavage, *Angew. Chem., Int. Ed.*, 2021, **60**, 11991–12000.
77 M. Westerhausen, Synthesis and spectroscopic properties of bis(trimethylsilyl)amides of the alkaline-earth metals magnesium, calcium, strontium, and barium, *Inorg. Chem.*, 1991, **30**, 96–101.
78 C. Bakewell, Magnesium hydrides bearing sterically demanding amidinate ligands: synthesis, reactivity and catalytic application, *Dalton Trans.*, 2020, **49**, 11354–11360.
79 J. Spielmann and S. Harder, Hydrocarbon-Soluble Calcium Hydride: A "Worker-Bee" in Calcium Chemistry, *Chem. – Eur. J.*, 2007, **13**, 8928–8938.
80 J. Brettar and S. Harder, Rational Design of a Well-Defined Soluble Calcium Hydride Complex, *Angew. Chem., Int. Ed.*, 2006, **45**, 3474–3478.
81 A. Causero, G. Ballmann, J. Pahl, C. Färber, J. Intemann and S. Harder, β-Diketiminate calcium hydride complexes: the importance of solvent effects, *Dalton Trans.*, 2017, **46**, 1822–1831.
82 P. Rinke, H. Görls, P. Liebing and R. Kretschmer, Synthesis and Characterization of Magnesium-Hydride Complexes with Alkylene-Bridged Bis(β-diketiminate) Ligands, *Organometallics*, 2023, **42**, 2287–2292.
83 P. Rinke, H. Görls and R. Kretschmer, Calcium and Magnesium Bis(β-diketiminate) Complexes: Impact of the Alkylene Bridge on Schlenk-Type Rearrangements, *Inorg. Chem.*, 2021, **60**, 5310–5321.
84 M. P. Coles, The role of the bis-trimethylsilylamido ligand, $[N\{SiMe_3\}_2]^-$, in main group chemistry. Part 1: Structural chemistry of the s-block elements, *Coord. Chem. Rev.*, 2015, **297–298**, 2–23.
85 A. D. Bage, K. Nicholson, T. A. Hunt, T. Langer and S. P. Thomas, The Hidden Role of Boranes and Borohydrides in Hydroboration Catalysis, *ACS Catal.*, 2020, **10**, 13479–13486.
86 A. D. Bage, T. A. Hunt and S. P. Thomas, Hidden Boron Catalysis: Nucleophile-Promoted Decomposition of HBpin, *Org. Lett.*, 2020, **22**, 4107–4112.
87 S. Mukhopadhyay, A. G. Patro, R. S. Vadavi and S. Nembenna, Coordination Chemistry of Main Group Metals with Organic Isocyanides, *Eur. J. Inorg. Chem.*, 2022, **2022**, e202200469.
88 A. P. Dove, P. Hormnirun, E. L. Marshall, J. A. Segal, A. J. P. White, D. J. Williams and V. C. Gibson, Low coordinate magnesium chemistry supported by a bulky β-diketiminate ligand, *Dalton Trans.*, 2003, 3088–3097, DOI: **10.1039/B303550F**.
89 S. Itsuno, C. Hachisuka, K. Kitano and K. Ito, Synthesis of secondary carbinamine via *n*-boryl imines generated from

nitriles and alkylboranes, *Tetrahedron Lett.*, 1992, **33**, 627–630.

90 H. C. Brown, P. Heim and N. M. Yoon, Selective reductions. XV. Reaction of diborane in tetrahydrofuran with selected organic compounds containing representative functional groups, *J. Am. Chem. Soc.*, 1970, **92**, 1637–1646.

91 F. Meger, A. C. W. Kwok, F. Gilch, D. R. Willcox, A. J. Hendy, K. Nicholson, A. D. Bage, T. Langer, T. A. Hunt and S. P. Thomas, B–N/B–H Transborylation: borane-catalysed nitrile hydroboration, *Beilstein J. Org. Chem.*, 2022, **18**, 1332–1337.

92 N. Matsumi and Y. Chujo, Synthesis of π-Conjugated Poly (cyclodiborazane)s by Organometallic Polycondensation, *Macromolecules*, 2000, **33**, 8146–8148.

93 Y. Chujo, I. Tomita and T. Saegusa, Hydroboration Polymerization of Dicyano Compounds. 4. Synthesis of Stable Poly(cyclodiborazane)s from Dialkylboranes, *Macromolecules*, 1994, **27**, 6714–6717.

94 M. Yalpani, R. Köster and R. Boese, Monomeric Aldiminodiorganoboranes and Aspects of Their Chemistry, *Chem. Ber.*, 1993, **126**, 285–288.

95 U. E. Diner, M. Worsley, J. W. Lown and J.-A. Forsythe, A novel asymmetric synthesis of α-aminoacids from nitriles employing diisopinocampheylborane as a chiral agent, *Tetrahedron Lett.*, 1972, **13**, 3145–3148.

96 M. F. Hawthorne, Amine boranes—X: Alkylideneamino t-butylboranes. The hydroboration of nitriles with trimethylamine t-butylborane, *Tetrahedron*, 1962, **17**, 117–122.

97 B. Okokhere-Edeghoghon, S. E. Neale, M. S. Hill, M. F. Mahon and C. L. McMullin, Isocyanate deoxygenation by a molecular magnesium silanide, *Dalton Trans.*, 2022, **51**, 136–144.

98 J. Burés, Variable Time Normalization Analysis: General Graphical Elucidation of Reaction Orders from Concentration Profiles, *Angew. Chem., Int. Ed.*, 2016, **55**, 16084–16087.

99 M. R. Crimmin, M. Arrowsmith, I. J. Casely, P. A. Procopiou, A. G. M. Barrett and M. S. Hill, Intramolecular Hydroamination of Aminoalkenes by Calcium and Magnesium Complexes: A Synthetic and Mechanistic Study, *J. Am. Chem. Soc.*, 2009, **131**, 9670–9685.

100 M. R. Crimmin, I. J. Casely and M. S. Hill, Calcium-Mediated Intramolecular Hydroamination Catalysis, *J. Am. Chem. Soc.*, 2005, **127**, 2042–2043.

101 M. Arrowsmith, M. R. Crimmin, A. G. M. Barrett, G. Kociok-Köhn, P. A. Procopiou and M. S. Hill, Cation Charge Density and Precatalyst Selection in Group 2-Catalyzed Aminoalkene Hydroamination, *Organometallics*, 2011, **30**, 1493–1506.

102 K. A. Johnson and R. S. Goody, The Original Michaelis Constant: Translation of the 1913 Michaelis–Menten Paper, *Biochemistry*, 2011, **50**, 8264–8269.

103 L. Michaelis and M. L. Menten, Die kinetik der invertinwirkung, *Biochem. Z.*, 1913, **49**, 352.

104 Y. Xia, H. Jiang and W. Wu, Recent Advances in Chemical Modifications of Nitriles, *Eur. J. Inorg. Chem.*, 2021, **2021**, 6658–6669.

105 (*a*) CCDC 2476567: Experimental Crystal Structure Determination, 2025, DOI: **10.5517/ccdc.csd.cc2p4286**; (*b*) CCDC 2476571: Experimental Crystal Structure Determination, 2025, DOI: **10.5517/ccdc.csd.cc2p42db**.